A novel RAD21 p.(Gln592del) variant expands the clinical description of Cornelia de Lange syndrome type 4 – review of the literature

Sanna Gudmundsson[1], Göran Annéren[1], Íñigo Marcos-Alcalde[2,3], Maria Wilbe[1], Malin Melin[1], Paulino Gómez-Puertas[2], Marie-Louise Bondeson[1]

[1]Department of Immunology, Genetics and Pathology, Uppsala University, Science for Life Laboratory, Uppsala, Sweden

[2]Centro de Biología Molecular "Severo Ochoa" (CSIC-UAM). 28049 Madrid, Spain

[3]Faculty of Experimental Sciences, Francisco de Vitoria University, Pozuelo de Alarcón, 28223 Madrid, Spain

Corresponding authors: Sanna Gudmundsson, e-mail: sanna.gudmundsson@igp.uu.se, +4618-4714806. Marie-Louise Bondeson, e-mail: marielouise.bondeson@igp.uu.se, +4618-611 5939. Address: Biomedical Center, Uppsala University, Box 815, 75108, Uppsala, Sweden.

CONFLICT OF INTEREST

The authors declare no conflicts of interest.

ABSTRACT

Cornelia de Lange syndrome (CdLS) is a heterogeneous developmental disorder where 70% of clinically diagnosed patients harbor a mutation in one of five CdLS associated cohesin proteins. Around 500 mutations have been identified to cause CdLS, however only eight different alterations are identified in *RAD21*, encoding the RAD21 cohesin protein that constitute the link between SMC1A and SMC3 within the cohesin ring. We report a 15-month-old boy presenting with developmental delay, distinct CdLS facial features, gastrointestinal reflux in early infancy, testis retention fetal pads and diaphragmatic hernia. Exome sequencing revealed a novel *RAD21* variant, c.1774_1776del; p.(Gln592del), suggestive of CdLS type 4. Segregation analysis of the two healthy parents confirmed the variant as *de novo* and bioinformatic analysis predicted the variant as disease-causing. Functional assessment by *in silico* structural model predicted that the p.Gln592del variant results in a discontinued contact between RAD21-Lys591 and the SMC1A residues Glu1191 and Glu1192, causing changes in the RAD21-SMC1A interface. In conclusion, we report a novel RAD21 p.(Glu592del) variant that expands the clinical description of CdLS type 4 and validate the pathogenicity of the variant by *in silico* structural modeling that displayed disturbed RAD21-SMC1A interface.

KEYWORDS

RAD21; Cornelia de Lange syndrome type 4; cohesin protein; cohesin complex

INTRODUCTION

Cornelia de Lange syndrome (CdLS) is characterized by cognitive impairment, growth deficiency, skeletal malformations, distinct facial features such as long eyelashes and arched eyebrows, and other major system deficiencies like gastrointestinal reflux. The patient group is heterogeneous with great variety in clinical manifestations and severity, primarily depending on which of the five CdLS associated cohesin proteins that are affected and the type of variant. Around 60% of clinically diagnosed patients with CdLS harbor a Nipped B-like (*NIPBL*) variant, which results in a sever CdLS phenotype. Approximately 5% are diagnosed with a Structural maintenance of chromosomes 1a (*SMC1A*) variant, 5% with a Histone deacetylase 8 (*HDAC8*) variant and less then 1% harbor a mutation in Structural maintenance of chromosome 3 (*SMC3*) or *RAD21*. About 500 mutations affecting the cohesin complex have been associated to CdLS. However, 30 % of CdLS patients are without a genetic diagnosis (Boyle et al., 2015) and so far, only eight different alterations in *RAD21* have been identified in CdLS type 4 patients (MIM #614701).

RAD21 (MIM 606462) was first associated to CdLS type 4 in four unrelated CdLS patients (Deardorff et al., 2012). Two patients had *de novo* deletions spanning *RAD21* (P1 and P4 in Figure 1D) and two patients had *de novo RAD21* missense mutations (c.1127C>G; p.Pro376Arg and c.1753T>C; p.Cys585Arg). Two previously reported patients diagnosed with Langer-Giedion syndrome were also highlighted as their clinical features overlapped with CdLS type 4 and they had deletions spanning *RAD21* (McBrien et al., 2008; Wuyts et al., 2002). In 2014, Minor *et al*. reported two patients, one with a *de novo* frameshift mutation (c.592_593dupAG; p.(Ser198Argfs*6)) of unknown origin and one patient with a maternally inherited deletion spanning exon 13. The mother displayed very mild CdLS features (Minor et al., 2014). Ansari *et al*. also reported a familial case where an unaffected father had passed on a splice donor mutation (c.274+1G>A) to his affected daughter (Ansari et al., 2014). In 2017,

Boyle *et al.* report a frameshift mutation, c.704delG; p.(Ser235Ilefs*19), in four female family members (Boyle et al., 2017) and Martínez *et al.* identified a *de novo* c.68G>A; p.(Trp23Ter) variant in a boy (Martinez et al., 2017) (Figure 1E). The RAD21 protein form the cohesin ring by linking the SMC1A and SMC3 head domains, that preserve the sister chromatids connected during cell division (Nasmyth and Haering, 2009). The cohesin ring is disrupted during anaphase by cleavage of RAD21 with active separase, allowing separation of the chromatids (Figure 1C) (Lin et al., 2016). Thus, the cohesin complex also serves an important function during transcriptional control and DNA-repair (Nasmyth and Haering, 2009).

Herein, we expand the clinical description of CdLS type 4 by reporting the clinical features of a 15-month-old boy with a novel mutation in RAD21. We also highlight the molecular effect of the variant by *in silico* structural modeling.

CLINICAL REPORT

The boy was born with normal birthweight (3460 g) into a family of two healthy parents and three healthy siblings. The boy presented with distinct facial morphology, microcephaly, developmental delay, growth delay, testicular retention and diaphragmatic hernia (which was surgically treated), as well as gastroesophageal reflux disease during infancy (Figure 1A; Table 1). No hearing impairment or malformations of distal limbs were noted but he displayed fetal pads on all fingers.

METHODS

Ethical consent

The study was performed according to the Declaration of Helsinki guidelines after approval by the local ethics committee, Uppsala (Dnr 2012/321) and collection of informed consent.

Whole-exome sequencing and segregation analysis

Clinical whole-exome sequencing (WES) and analysis protocols, developed by the Clinical genomics facility in Uppsala, were adapted as a clinical WES test at the Department of Clinical Genetics, Uppsala University Hospital, Sweden. Briefly, genomic DNA from the trio was extracted from peripheral blood using automated systems (EZ1 and QIAsymphony, QIAGEN) according to standard protocols. 250 ng of DNA was used for library preparation with Clinical Research Exome and SureSelectQXT Target Enrichment System (Agilent Technologies, Santa Clara, CA, USA). Sequencing was performed with 150 base pair long paired-end reads on a NextSeq500 sequencer (Illumina, San Diego, CA). Alignment of raw data to the human reference genome (GRCh37/hg19) was performed using BWA 0.7.10 and variant calling was performed with GATK haplotype caller (GATK framework 3.2.4, GenomeAnalysisTK 3.2.2) by using the Bcbio-Nextgen pipeline v 0.8.9 (https://github.com/chapmanb/bcbio-nextgen). Quality control parameters were calculated using FastQC 0.11.2, Picard HsMetrics 1.96 (http://broadinstitute.github.io/picard/) and GATK Depth of Coverage (GATK framework 3.2.4, GenomeAnalysisTK 3.2.2). For filtering of variants BenchLab NGS (Agilent Technologies, Inc.) was used. The allelic variants identified were classified according to the American College of Medical Genetics and Genomics and the Association for Molecular Pathology (Richards et al., 2015).

The selected variant was confirmed by Sanger sequencing of the family trio according to standard protocols (available upon request).

Three-dimensional structure modeling

The template structure was a stabilized model of human RAD21-Cterminal domain linked to the head domains of human SMC1A/SMC3 heterodimer, which was based on the structure of the C-terminal domain of yeast Scc1 protein (RAD21 in human) bound to yeast Smc1 homodimer (Protein Data Bank ID: 1W1W) (Haering et al., 2004), as previously described by Marcos-Alcalde *et al*. (Marcos-Alcalde et al., 2017). Model coordinates were built using the SWISS-MODEL server (http://swissmodel.expasy.org) and their structural quality was within the range of those accepted for homology-based structure (Anolea/Gromos/QMEAN4) (Benkert et al., 2011). To optimize geometries, the model was energy minimized using the GROMOS 43B1 force field implemented in DeepView (http://spdbv.vital-it.ch/), using 500 steps of steepest descent minimization followed by 500 steps of conjugate-gradient minimization. Figures were generated using the Pymol Molecular Graphics System (Schrödinger, LLC). Multiple sequence alignment of proteins from the RAD21 family was generated using TCOFFEE (http://www.tcoffee.org/) (Notredame et al., 2000).

RESULTS

Whole-exome sequencing revealed a novel *RAD21* c. 1774_1776del; p.(Gln592del) variant

Whole-exome sequencing was performed on the family trio with 93% of the reads mapping to the reference genome, at an average read depth of 159x and >10x for 97% of the exome in the index patient. Filtering of trio variants revealed heterozygosity for a novel *RAD21* variant, c.1774_1776del; p.(Gln592del), chr8:117859859_117859861delTTG (NM_006265) that was

confirmed *de novo* in the index patient (Figure 1B). The variant is not reported in the population of ExAC, GnomAD or SweGen databases (Ameur et al., 2017; Lek et al., 2016). ExAC database revealed that the level of observed missense variants in *RAD21* is lower than expected (ExAC: z=2.76). Further, there is only one homozygous missense variant reported (p.Asp414Glu; rs75160167, n=3), and no homozygous loss-of-function variants reported in the population databases (GnomAD, ExAC and SweGen).

***In silico* modelling displayed changes in the p.Gln592del RAD21-SMC1A interface**

The p.Gln592del variant is located in the C-terminal of the last exon (14/14) within the SMC1A binding domain of RAD21 (Figure 1E; p.558-628). The three-nucleotide position of the variant is conserved (PhyloP score 4.2; Figure 2A) and the deletion is predicted to be deleterious (PROVEAN: -11.124) and disease causing (MutationTaster). Amino acids Gln592, Arg590 and Lys591 are located in a positively charged environment in close contact to the negatively charged residues Glu119 and Glu1192 from the head domain of SMC1A (Figure 2B, left). Deletion of Gln592 results in rearrangement of the surrounding residues. In particular, the structural model predicts a significant positional change of Lys591, now located in the space previously occupied by Gln592. As a result, the previous contact between Lys591 and the SMC1A residues Glu1191 and Glu1192 is discontinued, causing significant changes in the RAD21-SMC1A interface (Figure 2B, right).

Residues Arg590, Lys591 and Gln592 are located in the same alpha helix as Lys605 (Figure 2C, right). Lys605 is a key residue for the ATPase activity of the active site 1 of the cohesin ring, as it stabilizes the position of the SMC1A residues Asn35 and Gly35 in contact to ATP and the catalytic water molecule (Marcos-Alcalde et al., 2017). The changed interaction between RAD21 positive, and SMC1A negative, patches is suspected to generate a local disorganization of the interface, thus affecting p.Lys605 and subsequently the ATPase-dependent functionality of the cohesin head (Figure 2C, left).

DISCUSSION

We report clinical and genetic findings of a patient with CdLS type 4, a syndrome of which clinical features of only 13 patients have been described in the literature before (Table 1). The index patient presented with classical CdLS features as well as diaphragmatic hernia, which has been reported in about 1% of CdLS patients (Cunniff et al., 1993; Fryns, 1987; Jelsema et al., 1993; Marino et al., 2002; Pankau and Janig, 1993) but not in CdLS type 4 patients. Notably, the index patient presented with fetal pads that has been reported in a patient with a deletion spanning *RAD21* (McBrien et al., 2008) that shared clinical features with CdLS type 4 but was diagnosed with Langer-Giedion syndrome (Deardorff et al., 2012). In this report, we highlight that exostoses is most likely not associated to CdLS type 4 and *RAD21* mutations but caused by *EXTI* deletions. Exostoses has recurrently been associated to heterozygous stop and missense mutations in *EXT1* (MIM #133700) and has been reported in three CdLS patients (Deardorff et al., 2012; Pereza et al., 2015) with micro deletions spanning *EXT1* (Figure 1D).

The index patients was diagnosed with a novel *de novo RAD21* c.1774_1776, p.(Gln592del) variant. The affected p.Gln592 residue is conserved and the deletion is predicted as deleterious and disease-causing. Further, the p.Gln592del variant is not reported in publically available databases and missense variants in *RAD21* in the normal population are underrepresented, suggesting that variants in *RAD21* might be disease-causing. The lack of homozygous loss-of function variants in the normal population suggests that complete loss of RAD21 is lethal. Previously, eight unique heterozygous alterations of *RAD21* variants have been reported in patients affected with CdLS type 4; three missense mutations (Deardorff et al., 2012; Martinez et al., 2017), two frameshift mutations (Boyle et al., 2017; Minor et al., 2014), one in-frame deletion including exon 13 of *RAD21*, one splice donor mutation (Ansari

et al., 2014) and deletions spanning whole *RAD21* (Deardorff et al., 2012; Pereza et al., 2015). Deardorff *et al.* has also highlighted two previously published patients, with deletions spanning *RAD21*, diagnosed with Langer-Giedion syndrome but with clinical symptoms overlapping CdLS type 4 (McBrien et al., 2008; Wuyts et al., 2002).

The RAD21 cohesin complex protein serves an important function during the cell cycle as the cohesin ring keeps sister chromatids connected during S-phase, and cleavage of RAD21 during anaphase allows their separation. Deletion of *RAD21* has been shown to result in haploinsufficiency (reduced RAD21 RNA and protein levels) but a p.Pro376Arg variant did not affect the expression levels notably (Deardorff et al., 2012). Hence, different *RAD21* disease-causing variants suggestively act through different pathogenic mechanisms. It is clear that *RAD21* is sensitive to alterations and that variants can cause CdLS type 4, but there are also reports of heterozygous missense *RAD21* variants associated to CIPO (p.Ala622Thr) (Bonora et al., 2015) and autism spectrum disorder (p.(Phe114Leu)) (Yuen et al., 2015). The one-amino-acid deletion reported in this study is located in the N-terminal of RAD21 at the site responsible for coupling to the SMC1A-head (Haering et al., 2004). Functional analysis performed in this study by *in silico* modeling of RAD21 p.592del, display a clear structural change in residue Lys591 and, to a lesser extent, Arg590, which is predicted to affect the interface to SMC1A-head (Glu1191 and Glu1192). The p.592del variant is also suggested to influence RAD21 p.Lys605/Lys604 that facilitate a crucial function in ATP induced hydrolysis that is responsible for the opening of the cohesin molecule (Marcos-Alcalde et al., 2017). Therefore, we suggest that the function of the cohesin ring, and specifically the binding to SMC1A is altered, causing the phenotype observed in the patient.

In summary, we present a novel *RAD21* c.1774_1776del; p.(592del) variant, giving rise to CdLS type 4 in a 15-month-old boy. Segregation analysis, bioinformatic analysis, population data and *in silico* structural modeling vindicate the pathogenicity of the novel

variant. This report summarizes previously reported clinical manifestations of CdLS type 4 but also highlights new clinical symptoms, which will aid correct counseling of future CdLS type 4 patients.

ACKNOWLEDGMENTS

We would like to thank the family for participating in this study. The study was supported by grants from Uppsala University Hospital as well as grants from the Spanish Ministry of Economy, Industry and Competitiveness (contracts IPT2011-0964-900000 and SAF2011-13156-E to P.G-P). SG was supported by grants from the Sävstaholm foundation.

FIGURE TITLES AND LEGENDS

Figure 1: Overview of patient features and RAD21 properties. (A) The index patient presented with typical Cornelia de Lange syndrome phenotype. Parents and the three older siblings are healthy. (B) A novel *de novo* RAD21 p.(592del) variant was confirmed. (C) RAD21 (blue) serves as a link between SMC3 (green) and SMC1A (yellow) that form the cohesin ring, responsible for adhesion of the sister chromatids during cell division. The ring is disrupted during anaphase by cleavage of RAD21. The position of the p.Gln592del variant is indicated by a red arrow. (D) Three studies report deletions spanning *RAD21* in patients with Cornelia de Lange syndrome type 4 (black bars). Two patients with deletions spanning *RAD21* have been reported with Lager-Giedion syndrome (brown bars). (E) RAD21 is 631 amino acid long with three binding domains: SMC3 (green; p.1-103), STAG1/2 (purple; p.362-403) and SMC1A (yellow; p.558-628). Previously reported intragenic variants are marked as well as the novel p.(Gln592del) variant identified in the index patient (bold).

Figure 2: *In silico* modeling of Gln592del mutant. (A) Multiple sequence alignment display conservation of the C-terminal domain of RAD21 (colored according to BLOSUM62 score). Dots indicate RAD21 residues connecting with SMC1A (blue) and the position of the deletion, p.Gln592 (red). (B) Surface of the structure model for wild-type RAD21-Cterminal domain (left) and for RAD21-Cterminal domain with p.Gln592del (right) colored according to electrostatic characteristics (red: negative; blue: positive; white: neutral). Positively charged amino acid Arg590, interacting with SMC1A residue Glu1198, is affected by the p.Gln592 deletion. Lys591 has lost its connection to SMC1A residues Glu1191 and Glu1192. (C) Structure model for wild-type RAD21-Cterminal domain (left) and for RAD21-Ceterminal domain with p.Gln592del (right) with residues Arg590, Lys591, Gln592 and Lys605/Lys604* labeled. Lys591 residue have repositioned to the space previously occupied by the deleted Gln592 residue.

TABLES

Table 1: Clinical features reported in the index patient and/or >2 previously described Cornelia de Lange type 4 patients.

Clinical anomalies reported in >2 patients of different families, or in the index patient	Index patient	Previously reported patients (tot 13[†])
CdLS classical facial features		
synphrys	-	9
arched/thick/long eyebrows	+	12
long eyelashes	+	6
short nose with anteverted nostrils	+	9
broad or depressed nasal bridge	+	6
long philtrum	-	10
thin lips, down-turned corners	-	8
macrotia	+	7
ptosis	+	3
high or cleft palate	+	3
low set or/and posteriorly ears	+	3
micrognathia	+	2
developmental delay/ intellectual disability	+	13
microcephaly/ low occipitofrontal circumference	+	11
gastroesophageal reflux disease	+	7
sparse/fine/thin hair	+	3
short stature	+	3
genital abnormalities	+	*2*
fetal pads	+	*this report*
diaphragmatic hernia	+	*this report*
malformations of hand or fingers	-	10
5th finger clinodactyly	-	8
low birth weight/ decreased body weight	-	5
dislocated elbow/ abnormal extension	-	4
toe syndactyly	-	3
exostoses[‡]	-	3

[+] Observed in the index patient, II:1. [−] Not observed in the index patient. [†]Patient clinical features reported in >2 patients with different mutations [‡]Suggestively associated to *EXT1* deletions and not *RAD21* variants.

REFERENCES

Ameur, A., Dahlberg, J., Olason, P., Vezzi, F., Karlsson, R., Martin, M., Viklund, J., Kahari, A.K., Lundin, P., Che, H., Thutkawkorapin, J., Eisfeldt, J., Lampa, S., Dahlberg, M., Hagberg, J., Jareborg, N., Liljedahl, U., Jonasson, I., Johansson, A., Feuk, L., Lundeberg, J., Syvanen, A.C., Lundin, S., Nilsson, D., Nystedt, B., Magnusson, P.K., Gyllensten, U., 2017. SweGen: a whole-genome data resource of genetic variability in a cross-section of the Swedish population. Eur J Hum Genet.

Ansari, M., Poke, G., Ferry, Q., Williamson, K., Aldridge, R., Meynert, A.M., Bengani, H., Chan, C.Y., Kayserili, H., Avci, S., Hennekam, R.C., Lampe, A.K., Redeker, E., Homfray, T., Ross, A., Falkenberg Smeland, M., Mansour, S., Parker, M.J., Cook, J.A., Splitt, M., Fisher, R.B., Fryer, A., Magee, A.C., Wilkie, A., Barnicoat, A., Brady, A.F., Cooper, N.S., Mercer, C., Deshpande, C., Bennett, C.P., Pilz, D.T., Ruddy, D., Cilliers, D., Johnson, D.S., Josifova, D., Rosser, E., Thompson, E.M., Wakeling, E., Kinning, E., Stewart, F., Flinter, F., Girisha, K.M., Cox, H., Firth, H.V., Kingston, H., Wee, J.S., Hurst, J.A., Clayton-Smith, J., Tolmie, J., Vogt, J., Tatton-Brown, K., Chandler, K., Prescott, K., Wilson, L., Behnam, M., McEntagart, M., Davidson, R., Lynch, S.A., Sisodiya, S., Mehta, S.G., McKee, S.A., Mohammed, S., Holden, S., Park, S.M., Holder, S.E., Harrison, V., McConnell, V., Lam, W.K., Green, A.J., Donnai, D., Bitner-Glindzicz, M., Donnelly, D.E., Nellaker, C., Taylor, M.S., FitzPatrick, D.R., 2014. Genetic heterogeneity in Cornelia de Lange syndrome (CdLS) and CdLS-like phenotypes with observed and predicted levels of mosaicism. J Med Genet 51(10), 659-668.

Benkert, P., Biasini, M., Schwede, T., 2011. Toward the estimation of the absolute quality of individual protein structure models. Bioinformatics 27(3), 343-350.

Bonora, E., Bianco, F., Cordeddu, L., Bamshad, M., Francescatto, L., Dowless, D., Stanghellini, V., Cogliandro, R.F., Lindberg, G., Mungan, Z., Cefle, K., Ozcelik, T., Palanduz, S., Ozturk, S., Gedikbasi, A., Gori, A., Pippucci, T., Graziano, C., Volta, U., Caio, G., Barbara, G., D'Amato, M., Seri, M., Katsanis, N., Romeo, G., De Giorgio, R., 2015. Mutations in RAD21 disrupt regulation of APOB in patients with chronic intestinal pseudo-obstruction. Gastroenterology 148(4), 771-782 e711.

Boyle, M.I., Jespersgaard, C., Brondum-Nielsen, K., Bisgaard, A.M., Tumer, Z., 2015. Cornelia de Lange syndrome. Clin Genet 88(1), 1-12.

Boyle, M.I., Jespersgaard, C., Nazaryan, L., Bisgaard, A.M., Tumer, Z., 2017. A novel RAD21 variant associated with intrafamilial phenotypic variation in Cornelia de Lange syndrome - review of the literature. Clin Genet 91(4), 647-649.

Cunniff, C., Curry, C.J., Carey, J.C., Graham, J.M., Jr., Williams, C.A., Stengel-Rutkowski, S., Luttgen, S., Meinecke, P., 1993. Congenital diaphragmatic hernia in the Brachmann-de Lange syndrome. Am J Med Genet 47(7), 1018-1021.

Deardorff, M.A., Wilde, J.J., Albrecht, M., Dickinson, E., Tennstedt, S., Braunholz, D., Monnich, M., Yan, Y., Xu, W., Gil-Rodriguez, M.C., Clark, D., Hakonarson, H., Halbach, S., Michelis, L.D., Rampuria, A., Rossier, E., Spranger, S., Van Maldergem, L., Lynch, S.A., Gillessen-Kaesbach, G., Ludecke, H.J., Ramsay, R.G., McKay, M.J., Krantz, I.D., Xu, H., Horsfield, J.A., Kaiser, F.J., 2012. RAD21 mutations cause a human cohesinopathy. Am J Hum Genet 90(6), 1014-1027.

Fryns, J.P., 1987. [Posterolateral diaphragmatic hernia and Brachmann-de-Lange syndrome]. Arch Fr Pediatr 44(6), 474.

Haering, C.H., Schoffnegger, D., Nishino, T., Helmhart, W., Nasmyth, K., Lowe, J., 2004. Structure and stability of cohesin's Smc1-kleisin interaction. Mol Cell 15(6), 951-964.

Jelsema, R.D., Isada, N.B., Kazzi, N.J., Sargent, K., Harrison, M.R., Johnson, M.P., Evans, M.I., 1993. Prenatal diagnosis of congenital diaphragmatic hernia not amenable to prenatal or neonatal repair: Brachmann-de Lange syndrome. Am J Med Genet 47(7), 1022-1023.

Lek, M., Karczewski, K.J., Minikel, E.V., Samocha, K.E., Banks, E., Fennell, T., O'Donnell-Luria, A.H., Ware, J.S., Hill, A.J., Cummings, B.B., Tukiainen, T., Birnbaum, D.P., Kosmicki, J.A., Duncan, L.E., Estrada, K., Zhao, F., Zou, J., Pierce-Hoffman, E., Berghout, J., Cooper, D.N., Deflaux, N., DePristo, M., Do, R., Flannick, J., Fromer, M., Gauthier, L., Goldstein, J., Gupta, N., Howrigan, D., Kiezun, A., Kurki, M.I., Moonshine, A.L., Natarajan, P., Orozco, L., Peloso, G.M., Poplin, R., Rivas, M.A., Ruano-Rubio, V., Rose, S.A., Ruderfer, D.M., Shakir, K., Stenson, P.D., Stevens, C., Thomas, B.P., Tiao, G., Tusie-Luna, M.T., Weisburd, B., Won, H.H., Yu, D., Altshuler, D.M., Ardissino,

D., Boehnke, M., Danesh, J., Donnelly, S., Elosua, R., Florez, J.C., Gabriel, S.B., Getz, G., Glatt, S.J., Hultman, C.M., Kathiresan, S., Laakso, M., McCarroll, S., McCarthy, M.I., McGovern, D., McPherson, R., Neale, B.M., Palotie, A., Purcell, S.M., Saleheen, D., Scharf, J.M., Sklar, P., Sullivan, P.F., Tuomilehto, J., Tsuang, M.T., Watkins, H.C., Wilson, J.G., Daly, M.J., MacArthur, D.G., Exome Aggregation, C., 2016. Analysis of protein-coding genetic variation in 60,706 humans. Nature 536(7616), 285-291.

Lin, Z., Luo, X., Yu, H., 2016. Structural basis of cohesin cleavage by separase. Nature 532(7597), 131-134.

Marcos-Alcalde, I., Mendieta-Moreno, J.I., Puisac, B., Gil-Rodriguez, M.C., Hernandez-Marcos, M., Soler-Polo, D., Ramos, F.J., Ortega, J., Pie, J., Mendieta, J., Gomez-Puertas, P., 2017. Two-step ATP-driven opening of cohesin head. Sci Rep 7(1), 3266.

Marino, T., Wheeler, P.G., Simpson, L.L., Craigo, S.D., Bianchi, D.W., 2002. Fetal diaphragmatic hernia and upper limb anomalies suggest Brachmann-de Lange syndrome. Prenat Diagn 22(2), 144-147.

Martinez, F., Caro-Llopis, A., Rosello, M., Oltra, S., Mayo, S., Monfort, S., Orellana, C., 2017. High diagnostic yield of syndromic intellectual disability by targeted next-generation sequencing. J Med Genet 54(2), 87-92.

McBrien, J., Crolla, J.A., Huang, S., Kelleher, J., Gleeson, J., Lynch, S.A., 2008. Further case of microdeletion of 8q24 with phenotype overlapping Langer-Giedion without TRPS1 deletion. Am J Med Genet A 146A(12), 1587-1592.

Minor, A., Shinawi, M., Hogue, J.S., Vineyard, M., Hamlin, D.R., Tan, C., Donato, K., Wysinger, L., Botes, S., Das, S., Del Gaudio, D., 2014. Two novel RAD21 mutations in patients with mild Cornelia de Lange syndrome-like presentation and report of the first familial case. Gene 537(2), 279-284.

Nasmyth, K., Haering, C.H., 2009. Cohesin: its roles and mechanisms. Annu Rev Genet 43, 525-558.

Notredame, C., Higgins, D.G., Heringa, J., 2000. T-Coffee: A novel method for fast and accurate multiple sequence alignment. J Mol Biol 302(1), 205-217.

Pankau, R., Janig, U., 1993. Diaphragmatic defect in Brachmann-de Lange syndrome: a further observation. Am J Med Genet 47(7), 1024-1025.

Pereza, N., Severinski, S., Ostojic, S., Volk, M., Maver, A., Dekanic, K.B., Kapovic, M., Peterlin, B., 2015. Cornelia de Lange syndrome caused by heterozygous deletions of chromosome 8q24: comments on the article by Pereza et al. [2012]. Am J Med Genet A 167(6), 1426-1427.

Richards, S., Aziz, N., Bale, S., Bick, D., Das, S., Gastier-Foster, J., Grody, W.W., Hegde, M., Lyon, E., Spector, E., Voelkerding, K., Rehm, H.L., Committee, A.L.Q.A., 2015. Standards and guidelines for the interpretation of sequence variants: a joint consensus recommendation of the American College of Medical Genetics and Genomics and the Association for Molecular Pathology. Genet Med 17(5), 405-424.

Wuyts, W., Roland, D., Ludecke, H.J., Wauters, J., Foulon, M., Van Hul, W., Van Maldergem, L., 2002. Multiple exostoses, mental retardation, hypertrichosis, and brain abnormalities in a boy with a de novo 8q24 submicroscopic interstitial deletion. Am J Med Genet 113(4), 326-332.

Yuen, R.K., Thiruvahindrapuram, B., Merico, D., Walker, S., Tammimies, K., Hoang, N., Chrysler, C., Nalpathamkalam, T., Pellecchia, G., Liu, Y., Gazzellone, M.J., D'Abate, L., Deneault, E., Howe, J.L., Liu, R.S., Thompson, A., Zarrei, M., Uddin, M., Marshall, C.R., Ring, R.H., Zwaigenbaum, L., Ray, P.N., Weksberg, R., Carter, M.T., Fernandez, B.A., Roberts, W., Szatmari, P., Scherer, S.W., 2015. Whole-genome sequencing of quartet families with autism spectrum disorder. Nat Med 21(2), 185-191.

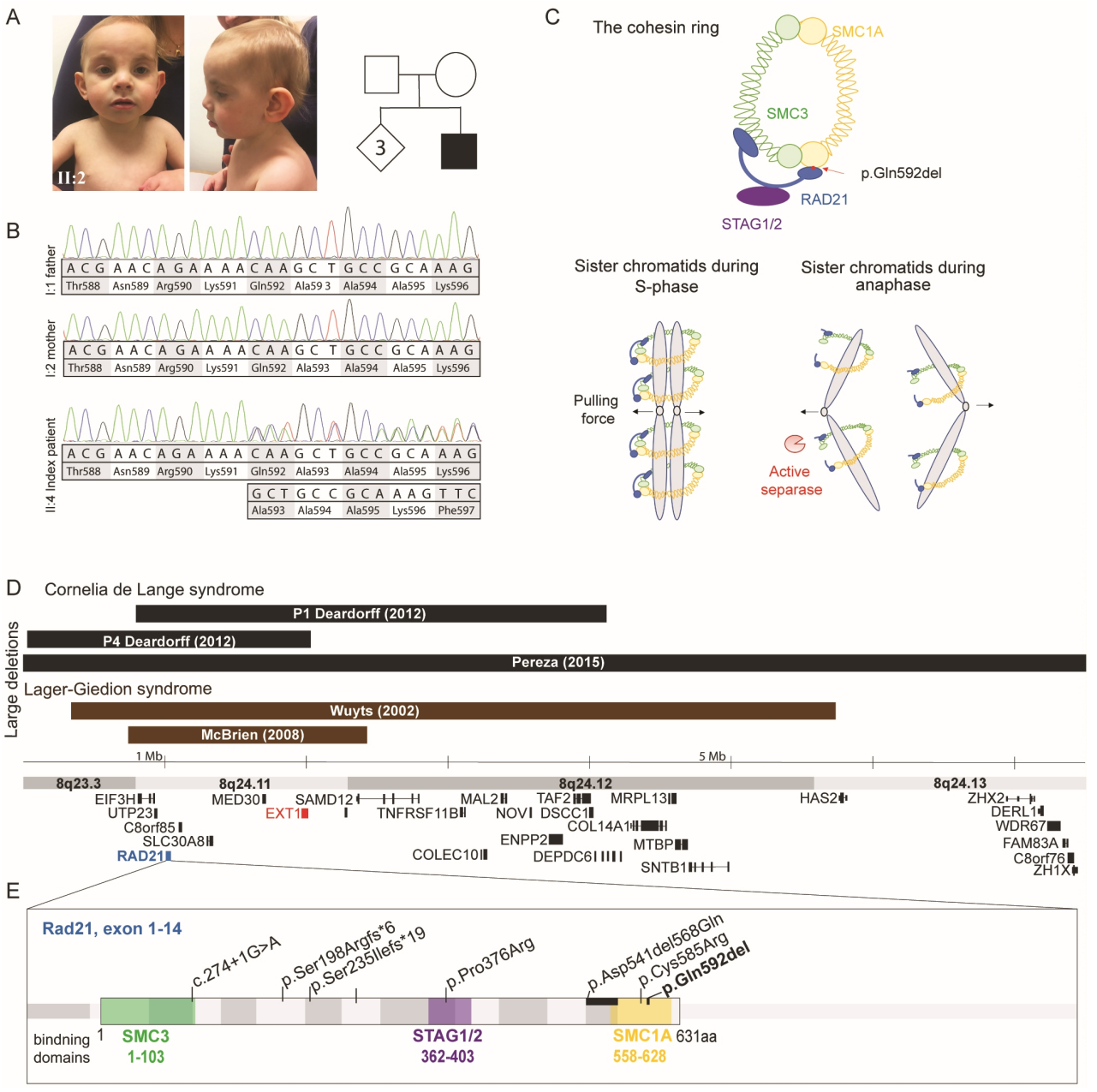
A
II:2
3
B
I:1 father
A C G A A C A G A A A C A A G C T G C C G C A A A G
Thr588 Asn589 Arg590 Lys591 Gln592 Ala59 3 Ala594 Ala595 Lys596
I:2 mother
A C G A A C A G A A A C A A G C T G C C G C A A A G
Thr588 Asn589 Arg590 Lys591 Gln592 Ala593 Ala594 Ala595 Lys596
II:4 Index patient
A C G A A C A G A A A C A A G C T G C C G C A A A G
Thr588 Asn589 Arg590 Lys591 Gln592 Ala593 Ala594 Ala595 Lys596
G C T G C C G C A A A G T T C
Ala593 Ala594 Ala595 Lys596 Phe597
C
The cohesin ring
SMC1A
SMC3
p.Gln592del
RAD21
STAG1/2
Sister chromatids during S-phase
Sister chromatids during anaphase
Pulling force
Active separase
D
Cornelia de Lange syndrome
P1 Deardorff (2012)
P4 Deardorff (2012)
Pereza (2015)
Large deletions
Lager-Giedion syndrome
Wuyts (2002)
McBrien (2008)
1 Mb
5 Mb
8q23.3
8q24.11
8q24.12
8q24.13
EIF3H
UTP23
C8orf85
SLC30A8
RAD21
MED30
SAMD12
EXT1
TNFRSF11B
MAL2
NOVI
TAF2
DSCC1
ENPP2
COLEC10
DEPDC6
MRPL13
COL14A1
MTBP
SNTB1
HAS2
ZHX2
DERL1
WDR67
FAM83A
C8orf76
ZH1X
E
Rad21, exon 1-14
c.274+1G>A
p.Ser198Argfs*6
p.Ser235Ilefs*19
p.Pro376Arg
p.Asp541del568Gln
p.Cys585Arg
p.Gln592del
bindning domains
1
SMC3
1-103
STAG1/2
362-403
SMC1A 631aa
558-628


A
SCC1_YEAST 475 -PTPG------EVASKAIVQMAKILRKELSEEKEVIFTDVLKSQANTEPENITKREASRGFFDILSLATEGCIGLSQTEAFGNIKIDAKPALF 560
SCC1_CAEEL 531 FGNTSTYKEDDGKWAKRAKHILKKVSADIETSGQADF------S-SVT-ATAKNRKQAAEQFYSLLILAKSQAISVDQSEPYGEIVIRPGANFK 616
RAD21_DANRE 555 EGQGGDQDQEERRWNKRTQQMLHGLQRVVAKTGAQSI------S-LLELCRNNNKKQAAAKFYSFLVLKKQQAIDLTQTEPYSDIIAAPGPRFH 624
RAD21_BOVIN 542 DASGGDQDQEERRWNKRTQQMLHGLQRALAKTGAESI------S-LLELCRNTNRKQAAAKFYSFLVLKKQQAIELTQEEPYSDIIATPGPRFH 628
RAD21_MOUSE 547 DASGGDQDQEERRWNKRTQQMLHGLQRALAKTGAESI------S-LLELCRNTNRKQAAAKFYSFLVLKKQQAIELTQEEPYSDIIATPGPRFH 633
RAD21_HUMAN 543 DASGGDQDQEERRWNKRTQQMLHGLQRALAKTGAESI------S-LLELCRNTNRKQAAAKFYSFLVLKKQQAIELTQEEPYSDIIATPGPRFH 629

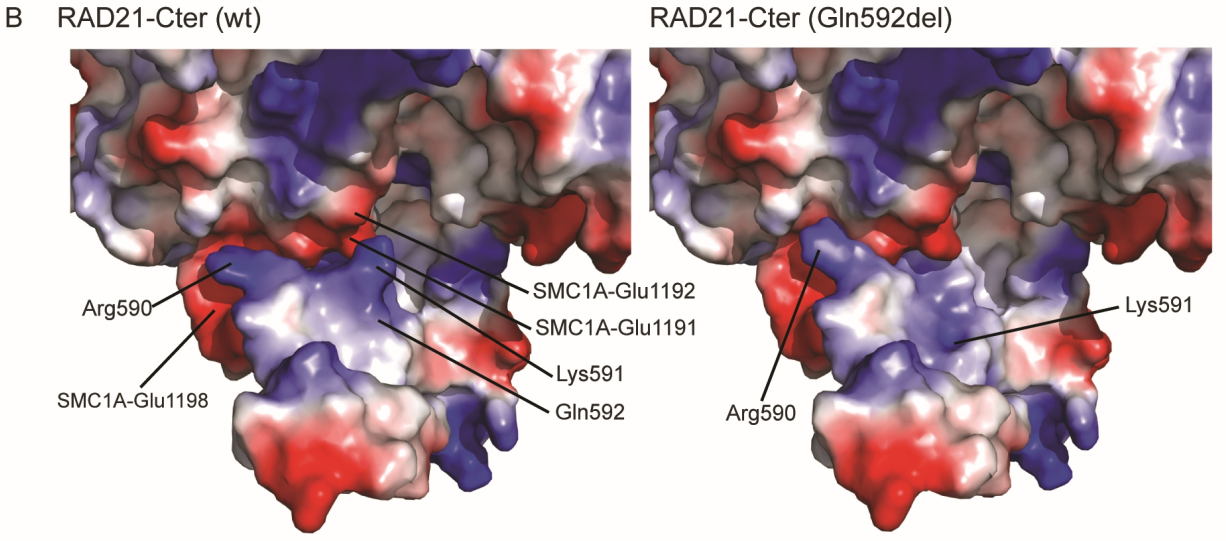
B
RAD21-Cter (wt)
RAD21-Cter (Gln592del)
Arg590
SMC1A-Glu1198
SMC1A-Glu1192
SMC1A-Glu1191
Lys591
Gln592
Arg590
Lys591

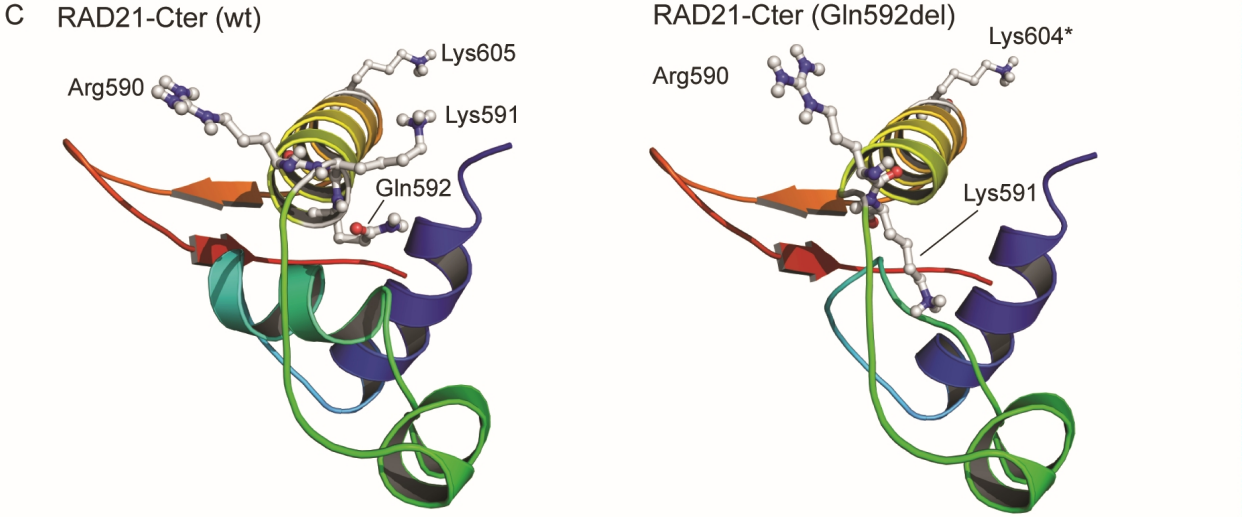
C
RAD21-Cter (wt)
RAD21-Cter (Gln592del)
Arg590
Lys605
Lys591
Gln592
Arg590
Lys604*
Lys591